Accepted Manuscript

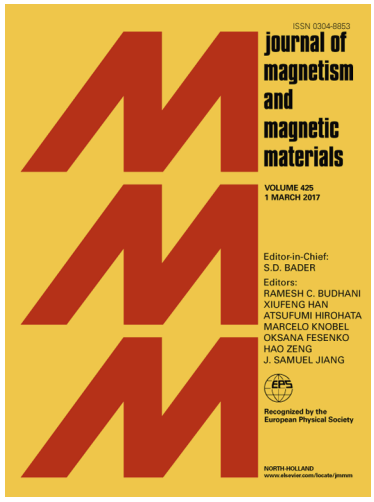

Short and long range ordering in $La_{1-x}Sr_xCoO_3$ cobaltites

Phan The Long, T.A. Ho, N.V. Quang, S.L. Cho, S.C. Yu

PII: S0304-8853(18)31581-6
DOI: https://doi.org/10.1016/j.jmmm.2019.01.010
Reference: MAGMA 64813

To appear in: *Journal of Magnetism and Magnetic Materials*

Received Date: 24 May 2018
Revised Date: 29 November 2018
Accepted Date: 2 January 2019

Please cite this article as: P.T. Long, T.A. Ho, N.V. Quang, S.L. Cho, S.C. Yu, Short and long range ordering in $La_{1-x}Sr_xCoO_3$ cobaltites, *Journal of Magnetism and Magnetic Materials* (2019), doi: https://doi.org/10.1016/j.jmmm.2019.01.010

This is a PDF file of an unedited manuscript that has been accepted for publication. As a service to our customers we are providing this early version of the manuscript. The manuscript will undergo copyediting, typesetting, and review of the resulting proof before it is published in its final form. Please note that during the production process errors may be discovered which could affect the content, and all legal disclaimers that apply to the journal pertain.

ACCEPTED MANUSCRIPT

Short and long range ordering in $La_{1-x}Sr_xCoO_3$ cobaltites

Phan The Long[1,2*], T. A. Ho[3], N. V. Quang[4], S. L. Cho[4], S. C. Yu[5]

[1]Laboratory of Magnetism and Magnetic Materials, Advanced Institute of Materials Science, Ton Duc Thang University, Ho Chi Minh City, Vietnam

[2]Faculty of Applied Sciences, Ton Duc Thang University, Ho Chi Minh City, Vietnam

[3]Department of Materials Science and Engineering, Korea University, Seoul 136-713, South Korea

[4]Department of Physics, University of Ulsan, Ulsan 680-749, South Korea

[5]Department of Physics, Chungbuk National University, Cheongju 361-763, South Korea

Abstract

We have carefully studied the relation between the critical and electrical behavior of rhombohedral $La_{1-x}Sr_xCoO_3$ (x = 0.2-0.5) compounds prepared by solid-state reactions. The results obtained from analyzing $M(T, H)$ data indicate that and all compounds undergo a second-order phase transition and the ferromagnetic-paramagnetic (FM-PM) transition temperature increase from approximate 182 K for x = 0.2 to 253 K for x = 0.5. Basing on the modified Arrott and Kouvel-Fisher techniques, scaling hypothesis, and critical isotherm analysis, we have determined the critical exponent values characteristic of magnetic order of $La_{1-x}Sr_xCoO_3$, with β = 0.361~0.489, γ = 1.021~1.346, and δ = 2.99~4.72. Interestingly, though all compounds are metallic ferromagnets, we have found the phase segregation in magnetic order as x > 0.3, where magnetic interactions tend to change from long-to-short-range FM order together with the absence of the insulating-like behavior at temperatures below 100 K. These phenomena are related to the spatial coexistence of multiple electronic and magnetic phases due to the changes in concentration of cobalt ions, spin-state transitions, and the existence of poor-hole anti-FM and hole-rich FM regions.

Keywords: Cobalt/cobalt compounds; magnetic materials/properties; electrical properties

*Corresponding author: phanthelong@tdtu.edu.vn

ACCEPTED MANUSCRIPT

1. Introduction

It is known that lanthanum cobalt oxide (cobaltite) in the stoichiometric form ($LaCoO_3$) has a rhombohedrally distorted perovskite structure. Its transport property is in the highly mixed character region between the Mott-Hubbard and charge-transfer insulators, and can change from an insulator through a semiconductor to the metallic behavior when temperature (T) increases [1-3]. Having studied its magnetic property, one has found a very complex scenario. For example, $LaCoO_3$ in the ground state is nonmagnetic (diamagnetic) with Co^{3+} in the low-spin (LS, $t_{2g}^6 e_g^o$, S = 0) configuration [4, 5], and there is the coexistence of the Curie-Weiss (CW) behaviour and Van-Vleck paramagnetism at temperatures T < 25 K [1] and the crossover of diamagnetic-paramagnetic transformation at ~100 K [6]. Additionally, $LaCoO_3$ undergoes the transition from a paramagnetic (PM) insulator to a PM metal above 500 K [6], which is different from lanthanum manganite ($LaMnO_3$) exhibiting only the insulating antiferromagnetic (AFM) behavior [7]. Such unusual magnetic and transport properties are ascribed to the spin-state transition of Co^{3+} from the LS configuration to intermediate-spin (IS, $t_{2g}^5 e_g^1$, S = 1) and high-spin (HS, $t_{2g}^4 e_g^2$, S = 2) configurations [2, 6, 8-10], and AFM superexchange interactions between Co^{3+} ions. These two spin states have very different features that the S = 1 state is Jahn-Teller active and accompanied with orbital degeneracy while the S = 2 state is not [11, 12]. A part from the impact of temperature, it has also been observed pressure- and field-driven spin-state transitions [9, 13, 14]. Stimulated by those intriguing properties, many research works have focussed on $LaCoO_3$ [9, 15, 16].

The magnetic and transport properties of $LaCoO_3$ could be remarkably improved if La^{3+} is partly replaced by a divalent element (Ca^{2+}, Ba^{2+}, or Sr^{2+}) [2, 17-21]. The doping creates more Co^{4+} ions, and hole-rich ferromagnetic (FM) metallic clusters (associated with the double-exchange interaction of Co^{3+}-Co^{4+} pairs) confined in the hole-poor insulating AFM matrix (associated with the super-exchange interaction of Co^{3+}-Co^{3+} and Co^{4+}-Co^{4+} pairs) [1, 2, 22]. Particularly, the introduction of charge carriers and Co^{4+} will increase the complexity of the system because it can

ACCEPTED MANUSCRIPT

also appear with LS ($t_{2g}^5 e_g^0$, S = 1/2), IS ($t_{2g}^4 e_g^1$, S = 3/2) and HS ($t_{2g}^3 e_g^2$, S = 5/2) states. By varying dopant content and external parameters (such as thermal energy, magnetic and electric fields, and pressure) [1-3, 5, 14, 22-24], one can easily control the strength of FM and AFM interactions, spin-state transitions, and magnetoelectric properties of hole-doped $LaCoO_3$ compounds as expected.

Among hole-doped $LaCoO_3$ compounds, $La_{1-x}Sr_xCoO_3$ has been of intensive interest because of showing the rich electrical and magnetic phase diagrams [1, 2] with intergranular giant magnetoresistance [11, 25, 26] and can be used as active catalysts for the water electrolysis in alkaline energy storage/conversion devices [27]. Concerning the electrical property, it has been found a gradual decrease in resistivity with increasing Sr content [2, 26]. Specifically, the compounds with $0 < x \leq 0.18$ have the insulating behavior, an insulating-metallic transition happens around x = 0.18, both insulating and metallic behaviors are available for $0.2 \leq x \leq 0.3$ (depending on temperature), and only the metallicity is for $0.3 < x \leq 0.5$ [1, 2, 10, 26]. Meanwhile, the magnetic phase diagram of $La_{1-x}Sr_xCoO_3$ is relatively simple that the spin-glass and cluster-glass (or FM-cluster) behaviors are revealed for $0.05 < x \leq 0.18$ and $0.18 \leq x \leq 0.5$, respectively. Because of the presence of the spin-glassy and FM-cluster states, it has been claimed that long-range FM order is absent in $La_{1-x}Sr_xCoO_3$ [1, 2, 11, 23, 28]. However, neutron-scattering studies have found a crossover from the short-range FM to long-range FM metallic state at a percolation threshold $x_p \approx$ 0.18 [26]. Some critical-behavior studies have also indicated long-range ferromagnetism in x = 0.21 and short-range FM state in other compositions [17-19, 29-31]. These results reflect a strong dependence of magnetic order on x. Unfortunately, the previous works on the critical behavior of $La_{1-x}Sr_xCoO_3$ only considered for one x value [18, 29-32] or a narrow range of x [17, 19]. Thus, it is difficult to follow the variation tendency of critical exponents as well as magnetic order with respect to x. Additionally, the previous studies have not taken into account the relation between the critical and electrical behaviors. To get more insight into those problems, we have prepared and studied the critical and electrical resistivity behaviors around the FM-PM phase transition temperature (T_C) of $La_{1-x}Sr_xCoO_3$ (x = 0.2-0.5) compounds with the robust Co^{3+}-Co^{4+} FM

ACCEPTED MANUSCRIPT

interactions. Though all compounds are metallic ferromagnets, we point out the phase segregation in magnetic ordering as $x > 0.3$, where magnetic interactions tend to change from long-range order to short-range order together with the absence of the insulating-like behavior at temperatures below 100 K. This work has also reviewed the results of the previous studies on the critical behavior of perovskike-type cobaltites.

2. Experimental details

Four polycrystalline cobaltite compounds of $La_{1-x}Sr_xCoO_3$ (x = 0.2, 0.3, 0.4, and 0.5) were prepared by the conventional solid-state reaction method. High-purity chemicals La_2O_3, $SrCO_3$ and Co_2O_3 in powder (99.9%) were used as precursors. These chemical combined with nominal compositions were well ground and mixed, and then calcinated in air at 1000 ^oC for 12 h. After several pre-annealing times at temperatures below 1200 ^oC, the obtained mixtures were re-ground and pressed into pellets by using a hydraulic lab press. These pellets were finally sintered at 1200 ^oC for 24 h. The room-temperature crystal structure of the final products was checked by a Rigaku X-ray diffractometer equipped with a Cu-$K\alpha$ radiation source with wavelength λ =1.5406 Å. Prior to taking X-ray powder diffraction (XRD) patterns, a small amount of standard Si powder was mixed with the compounds to minimize errors caused by the position calibration of X-ray incident angles. Magnetization measurements versus the temperature and magnetic field, $M(T, H)$, were performed on a superconducting quantum interference device (SQUID, Quantum Design, USA), according to the increasing direction of T and H, with temperature increments (ΔT) of 2 K around the FM-PM transition T_C and 5 K for other ranges.

3. Results and discussion

Fig. 1 shows room-temperature XRD patterns of all $La_{1-x}Sr_xCoO_3$ (x = 0.2-0.5) compounds. These patterns are fully Miller-indexed in the rhombohedral structure, belonging to the $R\bar{3}c$ space group. Rietveld refinement based on a rhombohedral structure model, as reported on the $La_{1-x}Sr_xCoO_3$ system in which Co occupies the *6b* site (0, 0, 0), La/Sr is in the *6a* site (0, 0, 0.25), and O is in the *18e* site (x, 0, 0.25) [3, 33, 34], provided a satisfactory fitting quality for each compound.

ACCEPTED MANUSCRIPT

The refined cell parameters (a_h, c_h, V_h, a_r and α_r), the Co-O bond length, and the Co-O-Co bond angle calculated for the compounds are shown in Table 1, where a_h and c_h refer to the lengths of the *a* and *c* axes in the hexagonal system, respectively, and a_r and α_r refer to the length of the *a* axis and the angle in the rhombohedral system, respectively. The variation tendency of these parameters are fairly the same as the results reported previously on $La_{1-x}Sr_xCoO_3$ [3, 24, 35], and explained due to the replacement of a larger Sr^{2+} ion (1.31 Å) for a smaller La^{3+} ion (1.16 Å), an increase in Co^{4+} concentration and created oxygen vacancies (V_O) or oxygen deficiency, leading to a decrease in Co^{3+} concentration, when *x* increases.

If more attention is given to the feature of XRD patterns, one can see the decreased splitting of XRD peaks versus increasing Sr content. Concerning this problem, it is known that the rhombohedral structure is a distorted type of an ideal cubic structure with the $Pm\bar{3}m$ space group resulted from a cooperative tilting of MnO_6 octahedra with the $a^-a^-a^-$ type, using Glazer's notation [36]. The rhombohedral distortion is characterized by splitting the Bragg single peaks of the cubic phase (with diffraction planes $(110)_c$, $(111)_c$, $(210)_c$ and $(211)_c$ peaked at $2\theta \approx 32.8$, 40.6, 53.2 and 58.68°, respectively) into several rhombohedral components, Fig. 1. The degree of the peak splitting would be decreased with increasing Sr content, implying that the Sr doping leads to a reduction of the rhombohedral distortion. On the other hand, the rhombohedral distortion degree can be also estimated via the rhombohedral angle α_r. As seen in Table 1, α_r decreases almost linearly from 60.58 for $x = 0.2$ to 60.21° for $x = 0.5$ and is expected to reach 60° at $x \geq 0.55$, which is related to the rhombohedral-cubic transformation [3, 35].

Fig. 2(a) shows zero-field-cooled (ZFC) and field-cooled (FC) $M(T)$ data of all $La_{1-x}Sr_xCoO_3$ compounds in an applied field $H = 100$ Oe. At a given *T* value in the FM phase, *M* increases with increasing Sr content. For the ZFC data, when temperature increases from 5 K, *M* also gradually increases and reaches the maximum at the so-called T_{max} (its value is listed in Table 1), where the anisotropic-field energy (generated by FM/AFM clusters) acting on magnetic moments of Co ions is equal to the energy of an applied field *H*. Under the FC condition, however, *M* tends to decrease

ACCEPTED MANUSCRIPT

when T increases from 5 K to T_{max}. There is also the bifurcation in the ZFC and FC curves at temperatures below the FM-PM transition temperatures (T_C). Such phenomena are widespread for both cobaltite and manganite systems, and dependent on the applied field magnitude [28, 37]. A temperature increase above T_{max} leads to the overlap of the ZFC and FC M curves and to a rapid decrease of M because of the FM-PM phase transition induced by thermal energy, where ordered magnetic moments become disordered. By plotting $dM(T)/dT$ curves, Fig. 2(b), we determined T_C values of 182, 229, 237, and 253 K for x = 0.2, 0.3, 0.4, and 0.5, respectively, in agreement with the results reported by Itoh et al [1]. If performing $\chi^{-1}(T) = H/M(T)$ curves for the PM region ($T > T_C$), the inset of Fig. 2(b), one can see clearly their linear variation obeying the CW law $\chi(T) = C/(T-\theta)$, where C and θ are the Curie constant and CW temperature, respectively. Fitting the $\chi^{-1}(T)$ data to the CW law at $T > T_C$ would obtain the values of C and θ. Similar to M, both T_C and θ (Table 1) also increase with increasing x. This is attributed to the enhanced FM correlation length and dynamic IS-LS exchange interactions mediated by the double-exchange between Co^{3+} and Co^{4+} ions [11, 12]. Based on the obtained C values and the relation $C = N(\mu_B \rho_{eff}^{exp})^2 / 3k_B$ (with Avogadro's number $N = 6.023\times10^{23}$ mol^{-1}, Bolzmann's constant $k_B = 1.3806\times10^{-23}$ J/K, and the Bohr magneton $\mu_B = 9.274\times10^{-24}$ J/T), we determined the effective PM moment (ρ_{eff}^{exp}). As shown in Table 1, ρ_{eff}^{exp} values are between 3 and 4, and fairly close to the theoretical values calculated according to the equation of $\rho_{eff}^{cal} = \sqrt{(1-x)\mu_{Co(3+)}^2 + x\mu_{Co(4+)}^2}$, where $\mu_{Co(3+)} \approx 2.83\,\mu_B$ and $\mu_{Co(4+)} \approx 3.87\,\mu_B$ are the effective magnetic moments of Co^{3+} and Co^{4+} ions, respectively, in the IS states. It should be noticed that the ρ_{eff}^{exp} values of $x \geq 0.4$ are quite different from those reported by Senarıs-Rodriguez and co-workers [2], but close to those reported by Xu and Muta et al [10, 35]. This could be due to different spin states of $Co^{3+,4+}$ ions and x-dependent Co^{3+}/Co^{4+} ratio, which are influenced by sample-preparation conditions and created V_O contents.

ACCEPTED MANUSCRIPT

To understand the Sr-doping influence on magnetic order in $La_{1-x}Sr_xCoO_3$, we have considered the initial magnetization, $M(H)$. Figs. 3(a-c) show the $M(H)$ data of typical compounds with x = 0.2, 0.4 and 0.5 recorded at temperatures around T_C. Similar to $M(T)$ data, Fig. 2(a), $M(H)$ also gradually decreases with increasing T. Additionally, with increasing H from 0 to 50 kOe, M increases nonlinearly at low temperatures, but becomes linear at high temperatures. No M saturation in all compounds has been achieved even at high-magnetic fields up to 50 kOe. Many cobaltites and manganites also exhibit these features [17, 18, 31, 38], which are related to magnetic inhomogeneities (due to FM clusters) and the FM-PM phase transition (where ordered magnetic moments of Co ions become disordered when T or thermal energy increases above T_C). Particularly, if performing H/M versus M^2 plots, Figs. 3(d-f), one can see that their slope is positive and there are no features like the H/M versus M^2 curves of $DyCo_2$ as $Er_{1-x}Pr_xCo_2$ compounds studied previously by Parra-Borderías et al [39]. According to Banerjee [40], the positive and positive slopes of H/M versus M^2 indicate first-order and second-order phase-transition characters, respectively. Based on those criteria, we suggest that our $La_{1-x}Sr_xCoO_3$ compounds have the character of a second-order phase transition (SOPT) and there is no token of a first-order (or even "weak" first-order) transition.

If observing carefully the features of H/M versus M^2 curves, Figs. 3(d-f), it comes to our attention that the variation tendency in slope around T_C is quite different and remarkably dependent on x in $La_{1-x}Sr_xCoO_3$. The x = 0.2 compound shows linear H/M versus M^2 curves at high fields and nonlinear parts at low fields, which are driven towards two opposite directions due to the FM-PM separation, Fig. 3(d). Meanwhile, the others (x = 0.4 and 0.5) do not show these features, Figs. 3(e, f). These different features are ascribed to different magnetic order of the compounds. The assessment of the difference in their magnetic order can be based on comparing the critical-exponent values of β, γ, and δ associated with temperature dependences of the spontaneous magnetization, $M_s(T)$, inverse initial susceptibility, $\chi_0^{-1}(T)$, and critical isotherm, $M(H)$ at T_C, respectively, with those of the standard models (the mean-field theory, tricritical mean-field, 3D Heisenberg and 3D Ising models). The determination of β, γ, and δ values is usually based on the

ACCEPTED MANUSCRIPT

theory of a "continuous" second-order phase transition proposed for a ferromagnet. According to Landau's theory [41], the free energy G_L for a FM system can be expressed as an expansion of M as $G_L = aM^2 + bM^4 + ... - HM$, where a and b are temperature-dependent coefficients. The equilibrium state is found at the minimum of G_L when $\partial G_L/\partial M$ is equal to zero, resulting in the Arrott-plot equation of $H/M = 2a + 4bM^2$ [42]. This equation can be generalized as the Arrott-Noakes equation of state, which is known in the modified Arrott (MA) method [43]

$$(H/M)^{1/\gamma} = c_1\varepsilon + c_2M^{1/\beta}, \qquad (1)$$

where c_1 and c_2 are temperature-dependent coefficients, and $\varepsilon = (T-T_C)/T_C$ is defined as the reduced temperature. Eq. (1) implies that with correct β and γ values the plot of $M^{1/\beta}$ versus $(H/M)^{1/\gamma}$ data in the vicinity of T_C introduces parallel straight lines and one of these lines passes through the origin at $T = T_C$. To estimate the β and γ values of the compounds, we firstly plotted the $M^{1/\beta}$ versus $(H/M)^{1/\gamma}$ curves with the exponents of the mean-field (MF, β = 0.5 and γ = 1.0), and 3D Heisenberg (β = 0.365 and γ = 1.336), 3D Ising (β = 0.325 and γ = 1.241), and tricritical MF (β = 0.25 and γ = 1) models [38, 44]. The preliminary checks indicated that the exponents of x = 0.2 and 0.3 are close to the MF theory values while those of x = 0.4 and 0.5 are close to the 3D-Heisenberg-model values. The exponent values of these two models are thus used as trial parameters for refining the correct β and γ values characteristic for $La_{1-x}Sr_xCoO_3$. This process is based on the MA method, using the following asymptotic relations

$$M_s(T) = M_0(-\varepsilon)^{\beta}, \qquad \varepsilon < 0, \qquad (2)$$

$$\chi_0^{-1}(T) = (h_0/M_0)\varepsilon^{\gamma}, \qquad \varepsilon > 0, \qquad (3)$$

where M_0 and h_0 are the critical amplitudes. As guided in detail by Kaul [45], with the selected trial exponents, $M_s(T)$ and $\chi_0^{-1}(T)$ data are determined from linear extrapolation for magnetization isotherms to $M^{1/\beta}$ and $(H/M)^{1/\gamma}$ (= $\chi_0^{-1})^{1/\gamma}$ axes, respectively. The $M_s(T)$ and $\chi_0^{-1}(T)$ data are then fitted to Eqs. (2) and (3), respectively, to achieve finer β and γ values. Concurrently, two T_C values

ACCEPTED MANUSCRIPT

extrapolated from the FM (M_s) and PM (χ_0^{-1}) regions would be the same. These β, γ, and T_C values will be used for the next MA processes until the critical parameters converge to their stable values. Fig. 4 shows the best fitting results, using the MA method for magnetic fields H > 10 kOe. We obtained β = 0.498(2), γ = 1.021(1) and T_C = 181 K for x = 0.2; β = 0.418(4), γ = 1.229(2) and T_C = 222 K for x = 0.3; β = 0.385(8), γ = 1.232(1) and T_C = 232 K for x = 0.4; and β = 0.361(1), γ = 1.346(4) and T_C = 244 K for x = 0.5, as listed in Table 2, the so-called MA exponents.

Alternatively, one can use the Kouvel-Fisher (KF) method to determine the exponent values through the following relations [46]

$$M_s(T)\cdot\left[\frac{dM_s(T)}{dT}\right]^{-1}=\frac{T-T_C}{\beta}, \tag{4}$$

$$\chi_0^{-1}(T)\cdot\left[\frac{d\chi_0^{-1}(T)}{dT}\right]^{-1}=\frac{T-T_C}{\gamma}. \tag{5}$$

It has been suggested that $M_s[dM_s/dT]^{-1}$ and $\chi_0^{-1}[d\chi_0^{-1}/dT]^{-1}$ versus T plots would introduce straight lines with slopes $1/\beta$ and $1/\gamma$, respectively. When these straight lines are extrapolated to the ordinate equal to zero, the intercepts on the T axis just correspond to T_C values [47]. As shown in Fig. 5 and Table 2, the best-fitting results as using the KF method introduce the critical values of β = 0.493(1), γ = 1.018(5) and T_C = 181 K for x = 0.2; β = 0.417(8), γ = 1.228(1) and T_C = 222 K for x = 0.3; β = 0.384(9), γ = 1.232(8)) and T_C = 232 K for x = 0.4; and β = 0.362(2), γ = 1.342(8) and T_C = 244 K for x = 0.5. These values (the so-called KF exponents) are very close to those determined from the MA method. Thus, the following will use the MA exponents for discussion.

With the β and γ values obtained from the MA and KF methods, we performed $M^{1/\beta}$ versus $(H/M)^{1/\gamma}$ curves. The results represented in Fig. 6 for the MA exponents indicate that $M^{1/\beta}$ versus $(H/M)^{1/\gamma}$ plots at temperatures around T_C give parallel straight lines (even at very low-magnetic fields) and one of these at T = T_C passes through the origin. According to the static-scaling

ACCEPTED MANUSCRIPT

hypothesis proposed in the scaling theory, the magnetization isotherms in the critical region is a ε- and H-dependent universal function as follows

$$M(H,\varepsilon) = |\varepsilon|^{\beta} \; f_{\pm}(H/|\varepsilon|^{\beta+\gamma}), \qquad (6)$$

where f_+ and f_- are regular functions for $T > T_C$ and $T < T_C$, respectively [38, 41, 47]. This equation means that by plotting M/ε^{β} versus $H/\varepsilon^{\beta+\gamma}$ with suitable β and γ values, all $M(H)$ data points at temperatures $T < T_C$ and $T > T_C$ would fall on the universal curves f_- and f_+, respectively. With the MA exponents and log-log scale plots shown in Fig. 7, all experimental data points fall on two universal curves, one for $T < T_C$ and the other for $T > T_C$. The same results are also observed for the exponents determined from the KF method, not shown here. For δ, its value can be obtained from the critical-isotherm (CI) relation $M(H, T_C) = DH^{1/\delta}$ or the Widom scaling relation $\delta = 1 + \gamma/\beta$ [38, 41], where D is the critical amplitude, and β and γ are the MA (or KF) exponent values obtained. As shown in Table 2, the δ values determined from both methods are almost the same, with $\delta \approx 3.0$, 3.9, 4.2, and 4.7 for x = 0.2, 0.3. 0.4, and 0.5, respectively. The analyses prove that the critical values obtained from the MA and KF methods are completely reliable and reflect frankly the magnetic nature of $La_{1-x}Sr_xCoO_3$ compounds.

Comparing with the theoretical values, Table 2, it comes to our attention that the exponents of x = 0.2 (β = 0.498 and γ = 1.021) are very close to those expected for the MF theory, fairly suitable to the results reported by Khan et al [17] on x = 0.21 with β = 0.485 and γ = 1.214. However, the scenario becomes more complex for other compounds (x = 0.3-0.5). While the β value of x = 0.3 (β = 0.418) is more MF-like, and that of x = 0.4 (β = 0.385) locates between those expected for the MF and 3D Heisenberg models, their γ values (= 1.229 and 1.232 for x = 0.3 and 0.4, respectively) are close to the value of the 3D Ising system (with γ = 1.241). Some authors have also found this critical fluctuation. As reported by Mira et al [19] on x = 0.2-0.3, β (= 0.43-0.46) is more MF-like, but γ (= 1.39-1.43) corresponds to the Heisenberg model. Meanwhile, Menyuk et al [32] studied x = 0.5 and found the γ = 0.27 value is close to the 3D Ising system, but δ = 3.05 is more MF-like. The

ACCEPTED MANUSCRIPT

nature of critical fluctuations could be due to the fact that β and γ are calculated from fitting the $M_s(T)$ and $\chi_0^{-1}(T)$ data below and above T_C, respectively. There could be room for other changes contributed to the FM-PM transition, such as the T-dependent spin-state change of Co ions [19] and the enhanced population of Jahn-Teller polarons due to the introduction of Co^{4+} [12]. Surprisingly, for the last compound (x = 0.5), its exponents (β = 0.361 and γ = 1.346) are close to those expected for the 3D Heisenberg model with nearest-neighbour FM interactions. If noticing the variation tendency of the exponents in our case, one can see a decrease of β together with an increase of γ and δ when x increases from 0.2 to 0.5. These results indicate that x = 0.2 has long-range FM order while x = 0.3-0.5 have short-range FM order. Magnetic order tends to decrease with increasing x. In other words, there is a phase separation in magnetic order in $La_{1-x}Sr_xCoO_3$ as $x \geq 0.3$, where magnetic interactions tend to change from long-range order to short-range order. As listed in Table 2, Saadaoui and Mukherjee et al [30, 31] also found short-range interactions in x = 0.4 and 0.5 with the exponents close to the 3D-Heisenberg system, fairly suitable to our results. For $La_{1-x}Ba_xCoO_3$ with $x \geq 0.3$ compounds, one also found short-range magnetic order with the exponents close to the 3D-Ising system [21]. However, many inconsistent results were reported on x = 0.2-0.3. For example, Khan et al [17, 18] found long-range FM order in x = 0.21 and short-range order in x = 0.25 and 0.33 while Mira et al [19] found only short-range order in x = 0.2-0.3. More recently, Li and co-workers [29] have found x = 0.3 exhibiting short-range interactions with the exponents (β = 0.272, γ = 1.291, and δ = 5.54) close to the 3D Ising system. These inconsistencies can be generated from several following causes:

(i) Oxygen stoichiometry in $La_{1-x}Sr_xCoO_3$, which is influenced by sample-preparation conditions, leading to different $Co^{3+,4+}$ concentrations and inhomogeneities, particularly for $x \geq 0.3$ [2, 3]. This was investigated by Zhang et al [48] for another cobaltite system of monoclinic $Pr_{0.5}Sr_{0.5}CoO_{3-\sigma}$, Table 2, where they found short-range and long-range FM order in the compounds with σ = 0 and 0.17, respectively.

ACCEPTED MANUSCRIPT

(ii) Studied sample types (single-crystal or polycrystalline samples) are different, because their critical behaviour is also dependent on magnetocrystalline anisotropy, size of crystallites/grains, and magnetic correlation length [18, 49].

(iii) The influences of the demagnetization field and magnetic-field ranges used for the MA (or KF) processes, as pointed out by Phan and Zhang et al [38, 49, 50] for the case of perovskite manganites.

We also believe that the long-to-short range-order transformation in $La_{1-x}Sr_xCoO_3$ compounds as $x \geq 0.3$ is tightly related to their electrical behavior. To clarify this problem, we have measured the electrical resistivity (ρ) of the compounds. The results recorded in the range T = 20-400 K reveal that they are all metallic ($\rho = 0.8\times10^{-3} \sim 4.5\times10^{-3}$ Ω.cm), and ρ decreases gradually with increasing x, owing to an enhancement of double-exchange interactions between Co^{3+} and Co^{4+} ions. The feature of $\rho(T)$ curves also indicates a phase separation as $x > 0.3$. Specifically, at $T < 100$ K, while only the metallicity was observed for x = 0.4 and 0.5, a metallic-insulating-like transition was observed for x = 0.2 and 0.3 at the so-called T_{MI} temperature (with $T_{MI} \approx 60$ and 86 K for x = 0.2 and 0.3, respectively). This phenomenon occurring at $T < T_{MI}$ could be related to spin-state transitions of Co ions and/or the inhomogeneity caused by the coexistence of poor-hole AFM and hole-rich FM phases [2]. At temperatures $T > 100$ K, though ρ of all compounds increases with increasing temperature, there is a change in slope ($S = d\rho/dT$) around T_C due to spin-disorder scattering, which has also been found in FM $SrRu_{1-x}Fe_xO_{3-\delta}$ materials [51]. Particularly, if considering the $S(T)$ curves, the inset of Fig. 8, one can see a rapid decrease of the maximum S around T_C when x increases above 0.3. With the results obtained from studying the critical behavior and $\rho(T)$, it is reasonable to claim the phase segregation in the magnetic and electrical properties in $La_{1-x}Sr_xCoO_3$ around x = 0.3, where magnetic order is driven from long-range type to short-range one accompanied with the loss of the insulator-like behavior (or the T_{MI} transition) at temperatures $T < 100$ K. It should be noticed that because x = 0.3 is at the boundary between short- and long-range ordering, its β value is more MF-like while γ is close to the 3D Ising system. Clearly, though

ACCEPTED MANUSCRIPT

$La_{1-x}Sr_xCoO_3$ has been known as spin-glass and cluster-glass (or FM-cluster) systems with the coexistence of poor-hole AFM and hole-rich FM regions [1, 2, 30], short- and long-range magnetic ordering could be still established. This is ascribed to the spatial coexistence of multiple electronic and magnetic phases, which are sensitive to the concentration and spin configurations of $Co^{3+,4+}$ ions. In fact, it has also been showed that long-range magnetic order could be established in complex spin structures, such as antiferomagnets and noncollinear magnets [52].

4. Conclusion

We prepared rhombohedral $La_{1-x}Sr_xCoO_3$ (x = 0.2-0.5) compounds by solid-state reactions, and studied their magnetic, critical, and electrical behaviors. The results revealed that all the compounds are metallic and exhibit the SOPT with T_C tuneable in the range of 181-253 K. Particularly, the results obtained from the critical behavior and $\rho(T)$ analyses indicated the magnetic and electrical phases taking place around x = 0.3, where there is the transition of long-range magnetic order (x = 0.2) to short-range one ($x \geq 0.3$) together with the disappearance of the insulator-like behavior at temperatures $T < T_{MI}$. The establishment of short- and long-range magnetic order in $La_{1-x}Sr_xCoO_3$ could be due to the spatial coexistence of multiple electronic and magnetic phases that are influenced by the concentration and spin-state changes of $Co^{3+,4+}$ ions.

Acknowledgements

The authors would like to thank Dr. K. W. Lee (Korea Research Institute of Standards and Science) for technical support when performing magnetic measurements on SQUID. This work was supported by a research grant from Ton Duc Thang University in 2019.

References

[1] M. Itoh, I. Natori, S. Kubota, K. Motoya, J. Phys. Soc. Jpn. 63 (1994) 1486.
[2] M.A. Señarís-Rodríguez, J.B. Goodenough, J. Solid Stat. Chem. 118 (1995) 323.
[3] A. Mineshige, M. Inaba, T. Yao, Z. Ogumi, K. Kikuchi, M. Kawase, J. Solid State Chem. 121 (1996) 423.
[4] M. Imada, A. Fujimori, Y. Tokura, Rev. Mod. Phys. 70 (1998) 1039.
[5] Q.M. Zhang, Q. Li, R.L. Gao, W.P. Zhou, L.Y. Wang, Y.T. Yang, D.H. Wang, L.Y. Lv, Y.W. Du, Appl. Phys. Lett. 104 (2014) 142409.
[6] J.B. Goodenough, J. Phys. Chem. Solids 6 (1958) 287.
[7] A.P. Ramirez, J. Phys.: Condens. Matter 9 (1997) 8171.

ACCEPTED MANUSCRIPT

[8] M.A. Korotin, S.Y. Ezhov, I.V. Solovyev, V.I. Anisimov, D.I. Khomskii, G.A. Sawatzky, Phys. Rev. B 54 (1996) 5309.
[9] A. Ikeda, T. Nomura, Y.H. Matsuda, A. Matsuo, K. Kindo, K. Sato, Phys. Rev. B 93 (2016) 220401(R).
[10] X. Xu, L. Jiang, J. Shen, Z. Chen, Z. Xu, Phys. Lett. A 351 (2006) 431.
[11] D. Phelan, D. Louca, S. Rosenkranz, S.-H. Lee, Y. Qiu, P.J. Chupas, R. Osborn, H. Zheng, J.F. Mitchell, J.R.D. Copley, J.L. Sarrao, Y. Moritomo, Phys. Rev. Lett. 96 (2006) 027201.
[12] D. Phelan, J. Yu, D. Louca, Phys. Rev. B 78 (2008) 094108.
[13] D.P. Kozlenko, N.O. Golosova, Z. Jirák, L.S. Dubrovinsky, B.N. Savenko, M.G. Tucker, Y. Le Godec, V.P. Glazkov, Phys. Rev. B 75 (2007) 064422.
[14] I. Fita, R. Szymczak, R. Puzniak, I.O. Troyanchuk, J. Fink-Finowicki, Y.M. Mukovskii, V.N. Varyukhin, H. Szymczak, Phys. Rev. B 71 (2005) 214404.
[15] N. Biškup, J. Salafranca, V. Mehta, M.P. Oxley, Y. Suzuki, S.J. Pennycook, S.T. Pantelides, M. Varela, Phys. Rev. Lett. 112 (2014) 087202.
[16] W.T. Hong, M. Gadre, Y.L. Lee, M.D. Biegalski, H.M. Christen, D. Morgan, S.H. Yang, J. Phys. Chem. Lett. 4 (2013) 2493.
[17] N. Khan, P. Mandal, K. Mydeen, D. Prabhakaran, Phys. Rev. B 85 (2012) 214419.
[18] N. Khan, A. Midya, K. Mydeen, P. Mandal, A. Loidl, D. Prabhakaran, Phys. Rev. B 82 (2010) 064422.
[19] J. Mira, J. Rivas, M. Vazquez, J.M.G. Beneytez, J. Arcas, R.D. Sanchez, M.A.S. Rodriguez, Phys. Rev. B 59 (1999) 123.
[20] T.L. Phan, T.V. Manh, T.A. Ho, D.Q. Viet, P. Zhang, S.C. Yu, Ceram. Int. 44 (2018) 15542.
[21] T.L. Phan, D.N. Petrov, J. Ćwik, N.T. Dang, D.Q. Viet, Current Appl. Phys. 18 (2018) 1248.
[22] A.P. Sazonov, I.O. Troyanchuk, H. Gamari-Seale, V.V. Sikolenko, K.L. Stefanopoulos, G.K. Nicolaides, Y.K. Atanassova, J. Phys.: Condens. Mat. 21 (2009) 156004.
[23] N.V. Khiem, N.X. Phuc, T.L. Phan, S.C. Yu, M.H. Phan, J. Appl. Phys. 97 (2005) 10A509.
[24] J. Mastin, M.-A. Einarsrud, T. Grande, Chem. Mater. 18 (2006) 6047.
[25] R. Mahendiran, A.K. Raychaudhuri, A. Chainanits, D.D. Sarma, J. Phys.: Condens. Matter 7 (1995) L561.
[26] J. Wu, J.W. Lynn, C.J. Glinka, J. Burley, H. Zheng, J.F. Mitchell, C. Leighton, Phys. Rev. Lett. 94 (2005) 037201.
[27] J.T. Mefford, X. Rong, A.M. Abakumov, W.G. Hardin, S. Dai, A.M. Kolpak, K.P. Johnston, K.J. Stevenson, Nature Communications 7 (2016) 1.
[28] D.N.H. Nam, K. Jonason, P. Nordblad, N.V. Khiem, N.X. Phuc, Phys. Rev. B 59 (1999) 4189.
[29] R. Li, P. Kumar, R. Mahendiran, J. Alloys Compd. 659 (2016) 203.
[30] S. Mukherjee, P. Raychaudhuri, A.K. Nigam, Phys. Rev. B 61 (2000) 8651.
[31] F. Saadaoui, R. M'nassri, H. Omrani, M. Koubaa, N. Chniba Boudjada, A. Cheikhrouhou, RSC Adv. 6 (2016) 50968.
[32] N. Menyuk, P.M. Raccah, K. Dwight, Phys. Rev. 166 (1968) 510.
[33] V.V. Sikolenko, E.V. Pomjakushina, S.Y. Istomin, J. Magn. Magn. Mater. 258-259 (2003) 300.
[34] V.V. Sikolenko, A.P. Sazonov, I.O. Troyanchuk, D. Többens, U. Zimmermann, E.V. Pomjakushina, H. Szymczak, J. Phys. Condens. Matter 16 (2004) 7313.
[35] K. Muta, Y. Kobayashi, K. Asai, J. Phys. Soc. Jpn. 71 (2002) 2784.
[36] A.M. Glazer, Acta Cryst. B 28 (1972) 3384.
[37] T.L. Phan, T.A. Ho, T.V. Manh, N.T. Dang, C.U. Jung, B.W. Lee, T.D. Thanh, J. Appl. Phys. 118 (2015) 143902.
[38] T.L. Phan, N.T. Dang, T.A. Ho, T.V. Manh, T.D. Thanh, C.U. Jung, B.W. Lee, A.T. Le, A.D. Phan, S.C. Yu, J. Alloys Compd. 657 (2016) 818.

ACCEPTED MANUSCRIPT

[39] M. Parra-Borderías, F. Bartolomé, J. Herrero-Albillos, L.M. García, J. Alloys Compd. 481 (2009) 48.
[40] S.K. Banerjee, Phys. Lett. 12 (1964) 16.
[41] H.E. Stanley, Introduction to phase transitions and critical phenomena, Oxford University Press, London, 1971.
[42] A. Arrott, Phys. Rev. 108 (1957) 1394.
[43] A. Arrott, J.E. Noakes, Phys. Rev. Lett. 19 (1967) 786.
[44] D. Kim, B. Revaz, B.L. Zink, F. Hellman, J.J. Rhyne, J.F. Mitchell, Phys. Rev. Lett. 89 (2002) 227202.
[45] S.N. Kaul, J. Magn. Magn. Mater. 53 (1985) 5.
[46] J.S. Kouvel, M.E. Fisher, Phys. Rev. 136 (1964) A1626
[47] J. Fan, L. Ling, B. Hong, L. Zhang, L. Pi, Y. Zhang, Phys. Rev. B 81 (2010) 144426.
[48] L. Zhang, J. Fang, J. Fan, M. Ge, L. Ling, C. Zhang, L. Pi, S. Tan, Y. Zhang, J. Alloys Compd. 588 (2014) 294.
[49] T.L. Phan, Y.D. Zhang, P. Zhang, T.D. Thanh, S.C. Yu, J. Appl. Phys. 112 (2012) 093906.
[50] P. Zhang, P. Lampen, T.L. Phan, S.C. Yu, T.D. Thanh, N.H. Dan, V.D. Lam, H. Srikanth, M.H. Phan, J. Magn. Magn. Mater. 348 (2013) 146.
[51] K.R.N. Toreh, D.H. Kim, U. Dash, T.L. Phan, B.W. Lee, H.W. Jin, S. Lee, B.H. Park, J.Y. Park, M.R. Cho, Y.D. Park, S.K. Acharya, W.S. Yoo, M.H. Jung, C.U. Jung, J. Alloys Compd. 657 (2016) 224.
[52] R. Skomski, Simple Models of Magnetism, Oxford University Press, New York, 2008.

ACCEPTED MANUSCRIPT

ACCEPTED MANUSCRIPT

Figure captions

Fig. 1. XRD data (symbols) of $La_{1-x}Sr_xCoO_3$ (x = 0.2-0.5) fitted to a theoretical model by using the Rietveld method (solid lines).

Fig. 2. (a) ZFC and FC $M(T)$ and (b) $dM(T)/dT$ curves for all $La_{1-x}Sr_xCoO_3$ compounds in an applied field H = 100 Oe. The inset shows ZFC $\chi^{-1}(T)$ data in the PM region fitted to the CW law.

Fig. 3. (a-c) $M(H)$ and (d-f) H/M versus M^2 curves of typical $La_{1-x}Sr_xCoO_3$ compounds with x = 0.2, 0.4 and 0.5.

Fig. 4. $M_s(T)$ and $\chi_0^{-1}(T)$ data are fitted to Eqs. (2) and (3), respectively, for typical $La_{1-x}Sr_xCoO_3$ compounds with (a) x = 0.2, (b) x = 0.4, and (c) x = 0.5.

Fig. 5. $M_s(T)$ and $\chi_0^{-1}(T)$ data are fitted to Eqs. (4) and (5), respectively, for typical $La_{1-x}Sr_xCoO_3$ compounds with (a) x = 0.2, (b) x = 0.4, and (c) x = 0.5.

Fig. 6. MA plots of $M^{1/\beta}$ versus $(H/M)^{1/\gamma}$ for $M(H)$ data of three typical compounds with (a) x = 0.2, (b) x = 0.4, and (c) x = 0.5, with exponent values β and γ obtained from the MAP method as described above. Temperature increments are fixed at 2 K.

Fig. 7. Scaling plots of $M/|\varepsilon|^{\beta}$ versus $H/|\varepsilon|^{\beta+\gamma}$ on a log-log scale for the $M(H)$ data of $La_{1-x}Sr_xCoO_3$ compounds with (a) x = 0.2, (b) x = 0.4, and (c) x = 0.5 around their FM-PM transition.

Fig. 8. Temperature dependences of the electrical resistivity, $\rho(T)$, of all $La_{1-x}Sr_xCoO_3$ compounds (x = 0.2-0.5). The inset shows the S variation with temperature (i.e., $d\rho/dT$ versus T) of the corresponding compounds around their T_C.

ACCEPTED MANUSCRIPT

Table 1. Experimental parameters of $La_{1-x}Sr_xCoO_3$ (x = 0.2-0.5) obtained from analysing the crystal structure, and $M(T)$ data for H = 100 Oe.

Compound	a_h (Å)	c_h (Å)	V (Å^3)	a_r (Å)	α_r (°)	Co-O (Å)	Co-O-Co (°)	T_{max} (K)	T_C (K)	θ (K)	ρ_{eff}^{exp} (μ_B)
x = 0.2	5.451(3)	13.180(1)	339.20(5)	5.404(3)	60.57(6)	1.937(4)	164.47(7)	152	182	196	3.36(7)
x = 0.3	5.446(2)	13.205(2)	339.21(7)	5.409(4)	60.45(1)	1.937(3)	164.49(7)	209	229	235	3.65(5)
x = 0.4	5.436(3)	13.226(3)	338.49(1)	5.411(8)	60.29(9)	1.936(5)	164.50(7)	219	237	245	3.82(8)
x = 0.5	5.425(4)	13.227(1)	337.19(4)	5.408(4)	60.20(8)	1.933(2)	164.51(3)	218	253	254	4.16(7)

ACCEPTED MANUSCRIPT

ACCEPTED MANUSCRIPT

Table 2. Critical parameters of our $La_{1-x}Sr_xCoO_3$ (x = 0.2-0.5) compounds compared with those reported previously on other single-crystal (SC) and polycrystalline (PC) perovskite-type cobaltites.

Compound	Technique	T_C (K)	β	γ	δ	Ref.
Mean-field model	Theory	-	0.5	1.0	3.0	[38]
3D Heisenberg model	Theory	-	0.365	1.336	4.66	[38]
3D Ising model	Theory	-	0.325	1.241	4.82	[38]
Tricritical mean-field model	Theory	-	0.25	1.0	5.0	[44]
$La_{0.8}Sr_{0.2}CoO_3$ (PC)	MA KF CI	181	0.498(2) 0.493(1)	1.021(1) 1.018(5)	3.04(4) 3.06(4) 2.99(1)	this work
$La_{0.7}Sr_{0.3}CoO_3$ (PC)	MA KF CI	222	0.418(4) 0.417(8)	1.229(2) 1.228(1)	3.94(2) 3.94(5) 3.83(2)	this work
$La_{0.6}Sr_{0.4}CoO_3$ (PC)	MA KF CI	232	0.385(8) 0.384(9)	1.232(1) 1.232(8)	4.19(4) 4.20(8) 3.96(5)	this work
$La_{0.5}Sr_{0.5}CoO_3$ (PC)	MA KF CI	244	0.361(1) 0.362(2)	1.346(4) 1.342(8)	4.72(9) 4.70(7) 4.39(3)	this work
$La_{0.8}Sr_{0.2}CoO_3$ (PC)	MA	199	0.46	1.39	4.02	[19]
$La_{0.75}Sr_{0.25}CoO_3$ (PC)	MA	222	0.46	1.39	4.02	[19]
$La_{0.7}Sr_{0.3}CoO_3$ (PC)	MA	223	0.43	1.43	4.38	[19]
$La_{0.79}Sr_{0.21}CoO_3$ (SC)	MA KF CI	188	0.485(2) 0.491(4)	1.214(4) 1.217(3)	3.50(1) 3.48(1) 3.51(1)	[17]
$La_{0.75}Sr_{0.25}CoO_3$ (SC)	MA KF CI	214	0.367(2) 0.362(2)	1.31(1) 1.304(6)	4.57(1) 4.60(1) 4.75(1)	[17]
$La_{0.67}Sr_{0.33}CoO_3$ (SC)	MA KF CI	223	0.363(2) 0.361(7)	1.315(1) 1.31(1)	4.62(1) 4.61(4) 4.64(1)	[17, 18]
$La_{0.7}Sr_{0.3}CoO_3$ (PC)	MA KF CI	227~228	0.270(7) 0.272(1)	1.282(2) 1.291(4)	5.75 5.75 5.54	[29]
$La_{0.6}Sr_{0.4}CoO_3$ (PC)	MA KF CI	230	0.396(4) 0.391(2)	1.320(1) 1.314(3)	4.330(2) 4.359(6) 4.761(1)	[31]
$La_{0.5}Sr_{0.5}CoO_3$ (PC)	MA KF CI	223	0.365 0.321(2)	1.336 1.351(9)	4.66 4.21 4.39(2)	[30]
$La_{0.5}Sr_{0.5}CoO_3$ (PC)	KF	228	-	1.27(2)	3.05(6)	[32]
$La_{0.3}Ba_{0.3}CoO_3$ (PC)	MA CI	192	0.328(1)	1.251(8)	4.81(4) 4.85(3)	[21]
$La_{0.5}Ba_{0.5}CoO_3$ (PC)	MA	153	0.331(2)	1.246(1)	4.76(4)	[21]

	CI				4.31(1)	
$Pr_{0.5}Sr_{0.5}CoO_3$ (PC)	MA KF CI	240	0.387(6) 0.391(9)	0.884(2) 0.971(7)	3.284(6) 3.483(9) 3.284(3)	[48]
$Pr_{0.5}Sr_{0.5}CoO_{2.83}$ (PC)	MA KF CI	160	0.516(8) 0.509(6)	0.993(6) 1.067(7)	2.92(4) 3.096(9) 3.046(2)	[48]

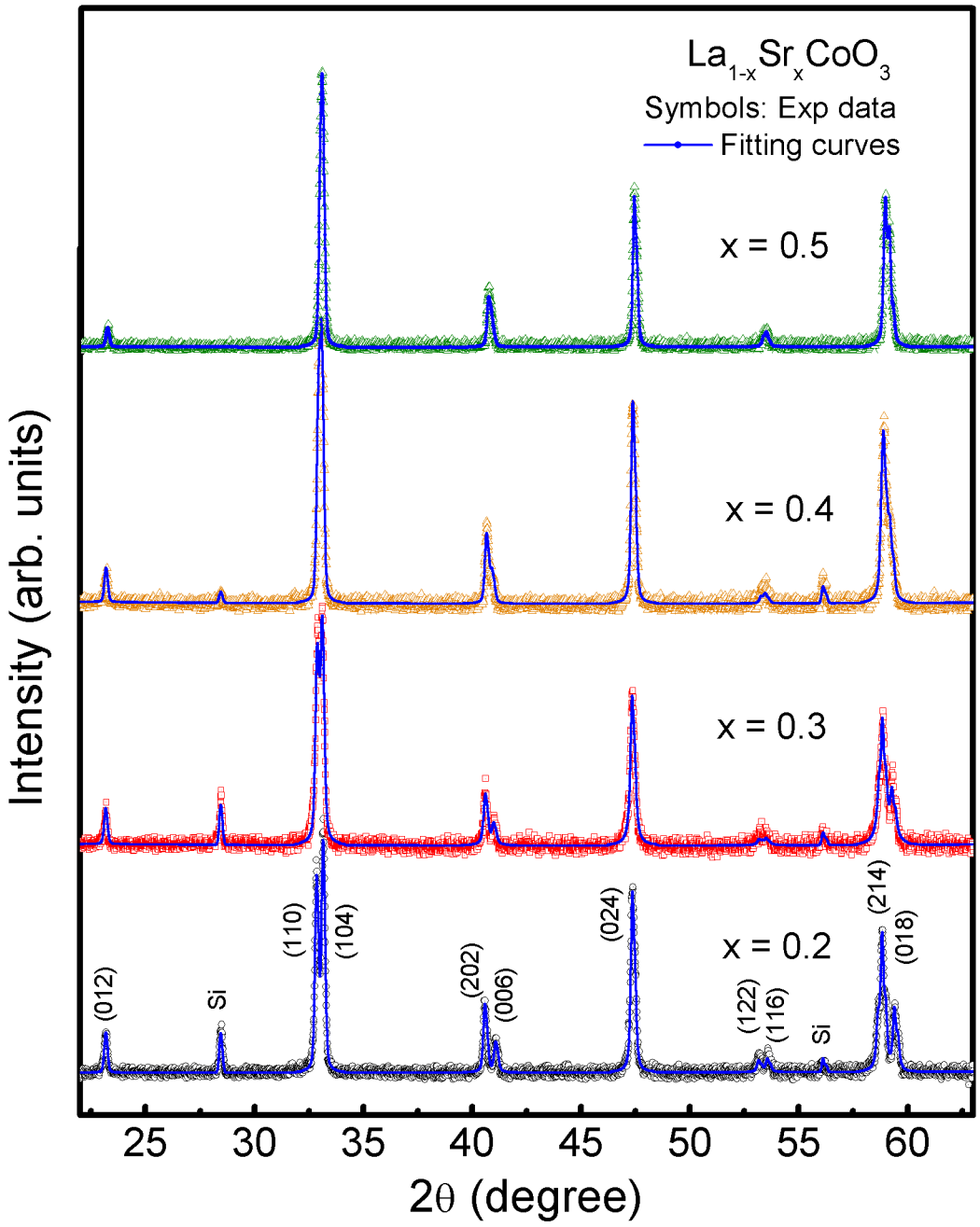

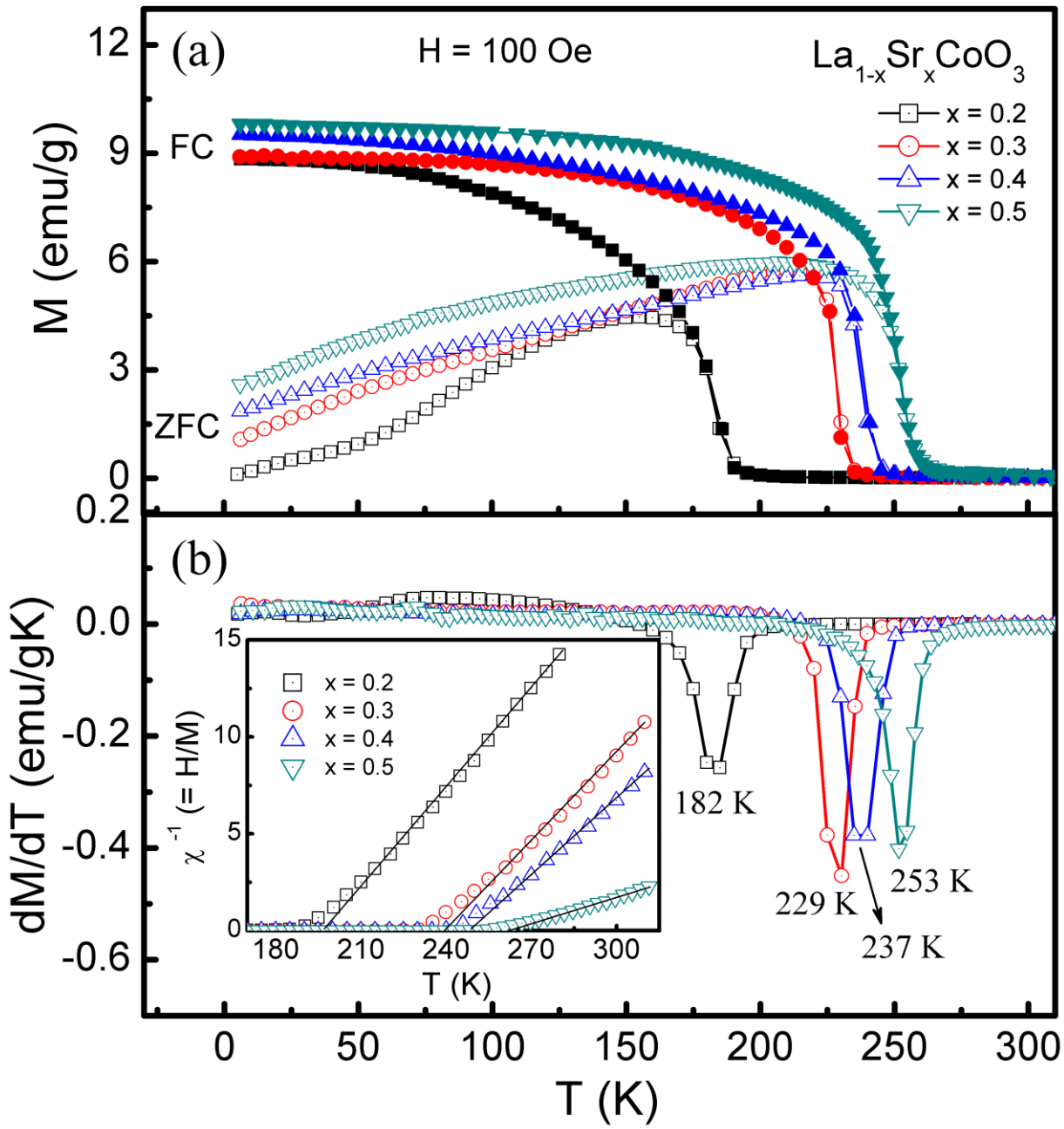
(a)
H = 100 Oe
La1-xSrxCoO3
x = 0.2
x = 0.3
x = 0.4
x = 0.5
FC
ZFC
M (emu/g)
12
9
6
3
0
0.2
(b)
dM/dT (emu/gK)
0.0
-0.2
-0.4
-0.6
χ-1 (= H/M)
15
10
5
0
180
210
240
270
300
T (K)
182 K
229 K
253 K
237 K
0
50
100
150
200
250
300
T (K)

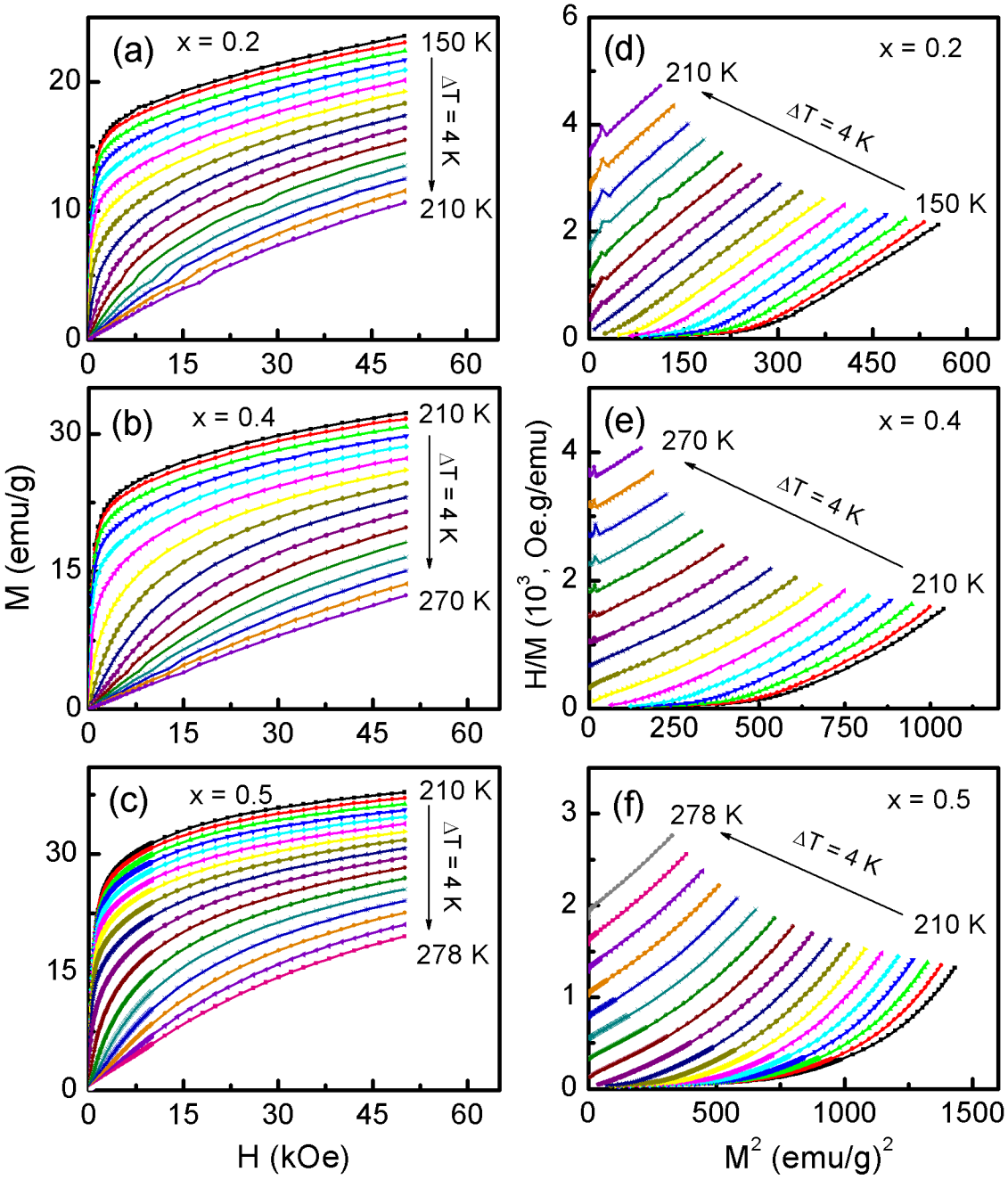
(a)
x = 0.2
150 K
ΔT = 4 K
210 K
(b)
x = 0.4
210 K
ΔT = 4 K
270 K
(c)
x = 0.5
210 K
ΔT = 4 K
278 K
M (emu/g)
H (kOe)
(d)
x = 0.2
210 K
ΔT = 4 K
150 K
(e)
x = 0.4
270 K
ΔT = 4 K
210 K
(f)
x = 0.5
278 K
ΔT = 4 K
210 K
H/M (10^3, Oe.g/emu)
M^2 (emu/g)^2

ACCEPTED MANUSCRIPT

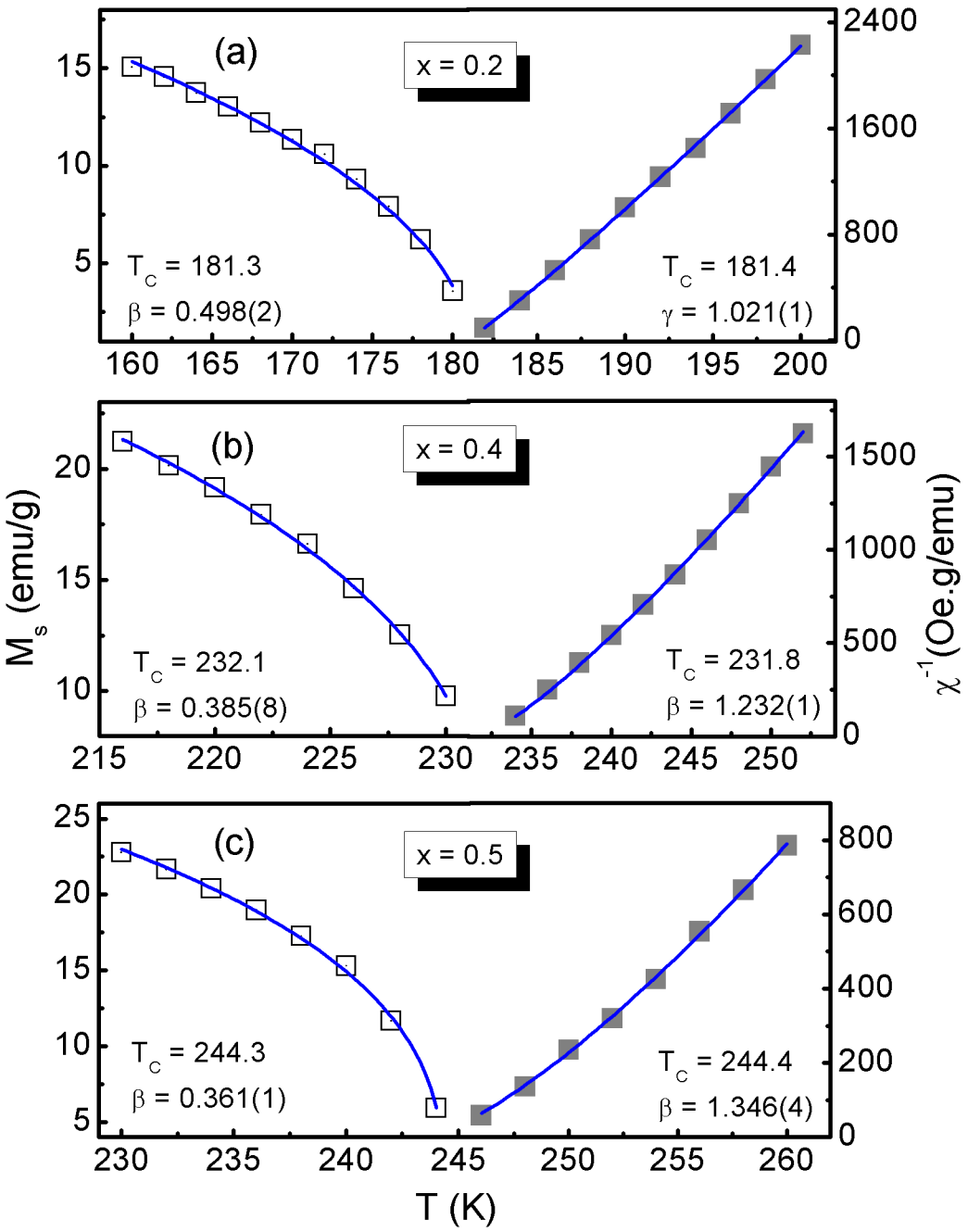

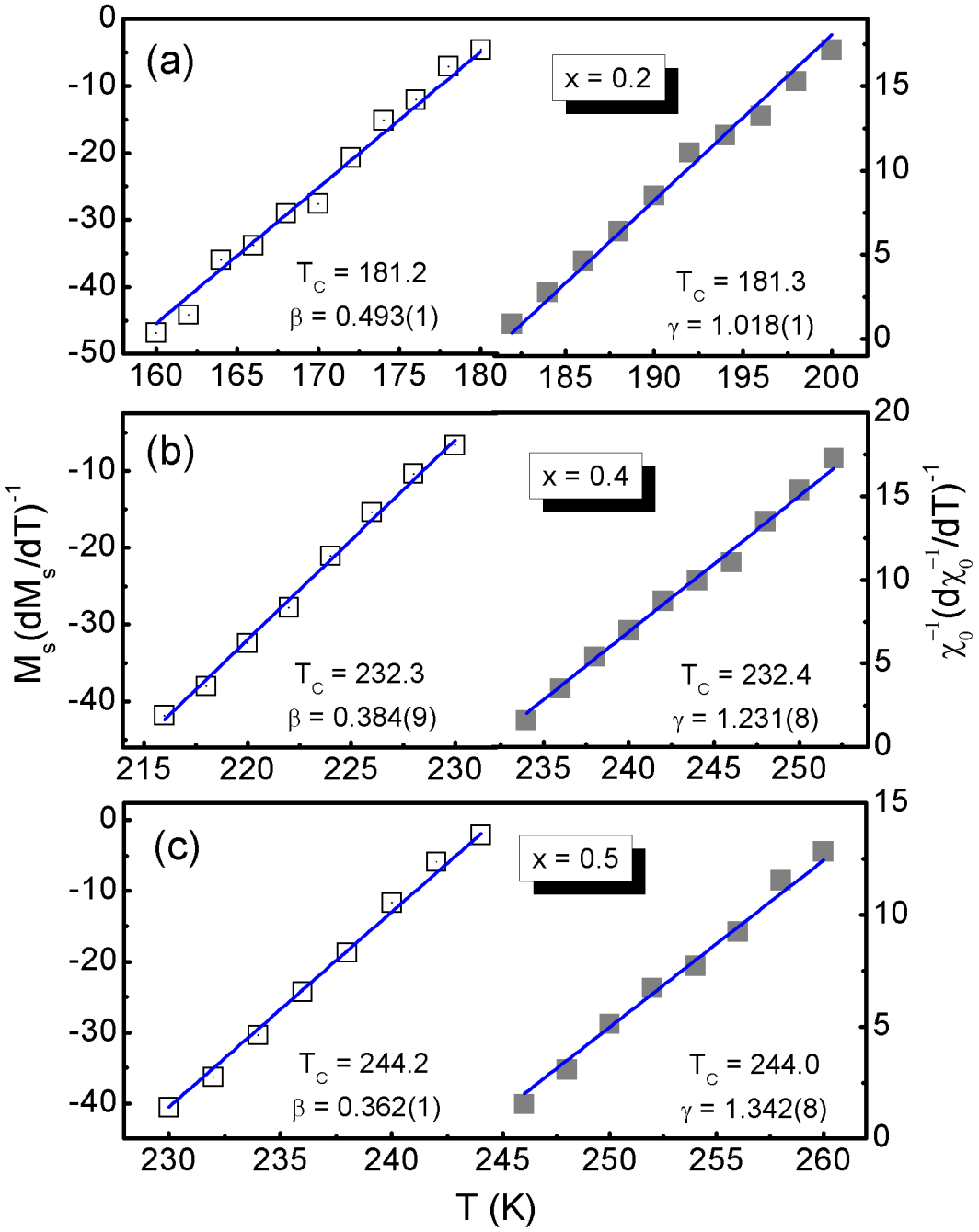
(a)
x = 0.2
T_C = 181.2
β = 0.493(1)
T_C = 181.3
γ = 1.018(1)
(b)
x = 0.4
T_C = 232.3
β = 0.384(9)
T_C = 232.4
γ = 1.231(8)
(c)
x = 0.5
T_C = 244.2
β = 0.362(1)
T_C = 244.0
γ = 1.342(8)
M_s(dM_s/dT)^-1
χ_0^-1(dχ_0^-1/dT)^-1
T (K)

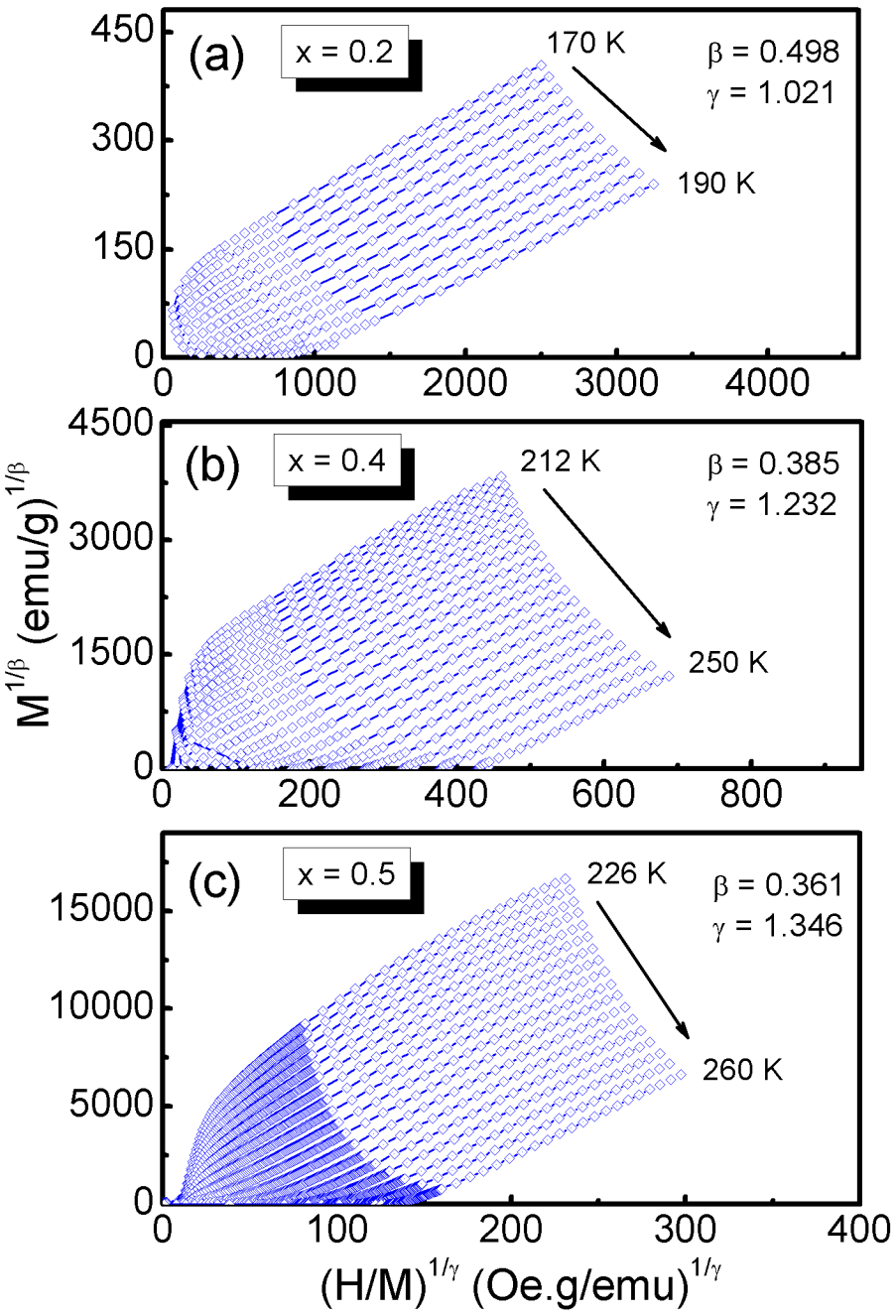
(a)
x = 0.2
170 K
190 K
β = 0.498
γ = 1.021
(b)
x = 0.4
212 K
250 K
β = 0.385
γ = 1.232
(c)
x = 0.5
226 K
260 K
β = 0.361
γ = 1.346
M^1/β (emu/g)^1/β
(H/M)^1/γ (Oe.g/emu)^1/γ

ACCEPTED MANUSCRIPT

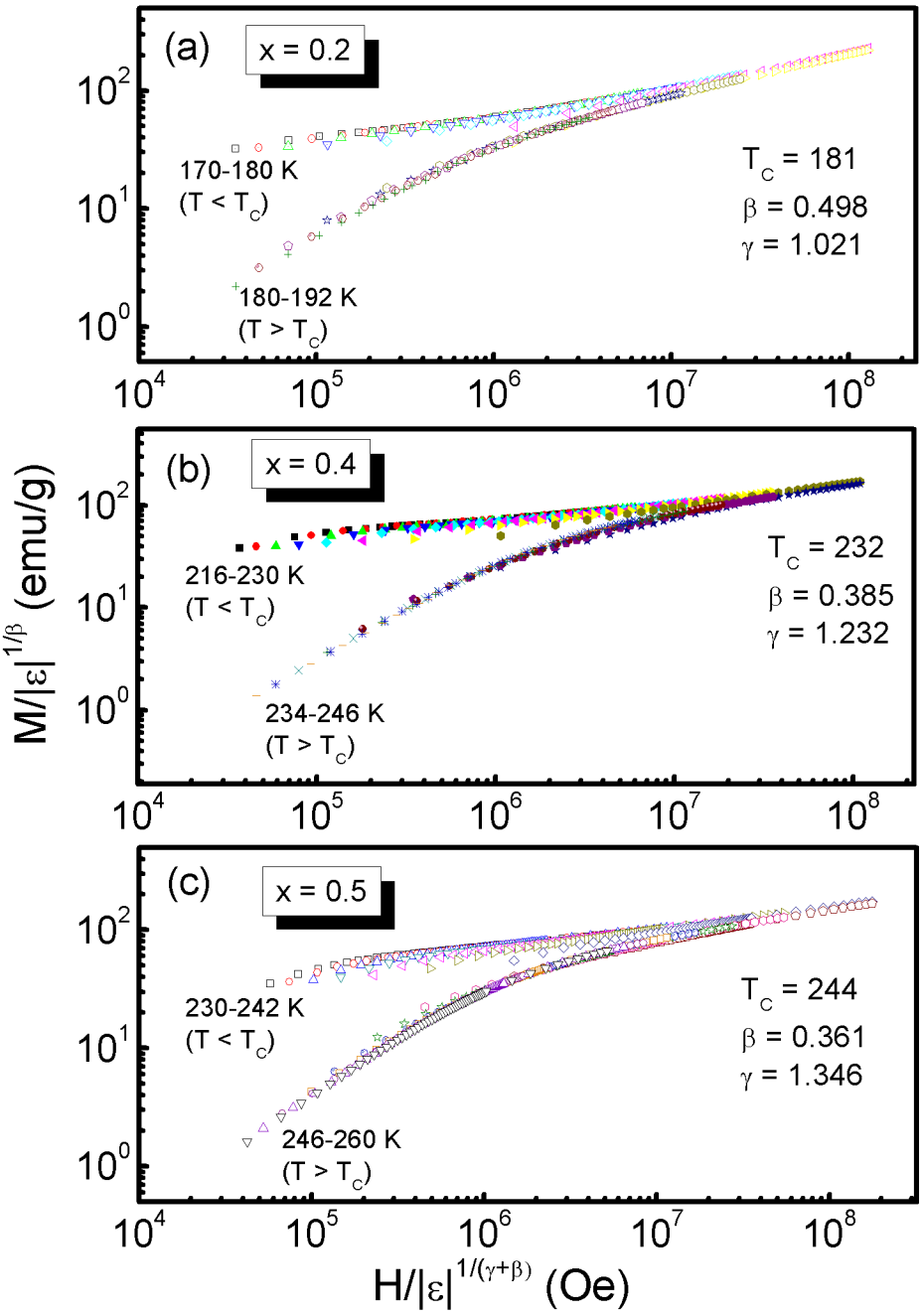

ACCEPTED MANUSCRIPT

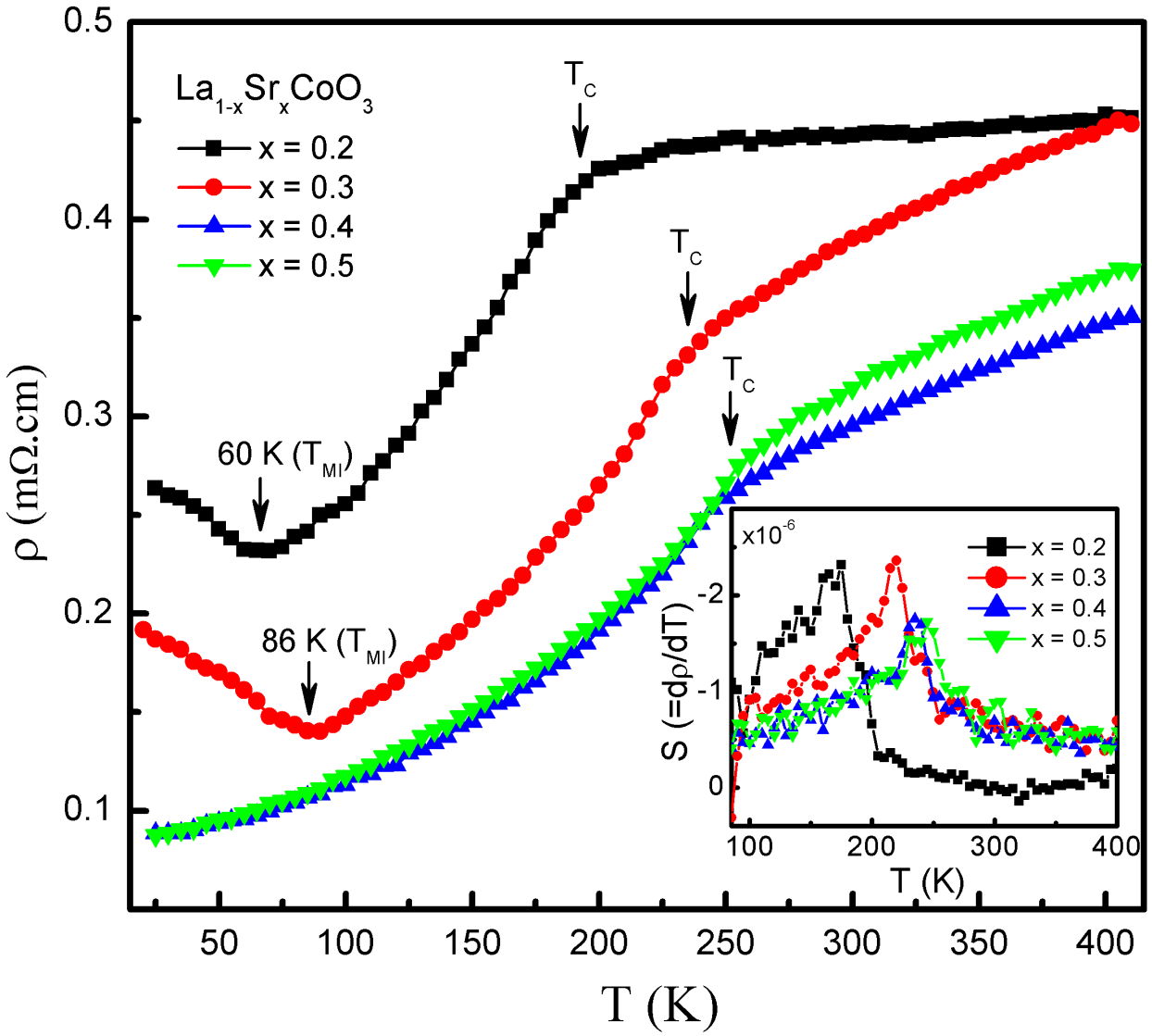

Highlights

- **The relation between critical and electrical behaviors in $La_{1-x}Sr_xCoO_3$**
- **Magnetic and electrical phase segregation in $La_{1-x}Sr_xCoO_3$ around $x = 0.3$**
- **A magnetic-order change from magnetic long-range order to short-range one as $x \geq 0.3$**
- **A careful review of critical behavior studies of perovskite cobaltites studied previously**

ACCEP